A 6-year analysis of stratospheric intrusions and their influence on ozone at Mt. Cimone (2165 m above sea level)

P. Cristofanelli,[1] P. Bonasoni,[1] L. Tositti,[2] U. Bonafè,[1] F. Calzolari,[1] F. Evangelisti,[1] S. Sandrini,[2] and A. Stohl[3]

Received 3 August 2005; revised 4 November 2005; accepted 18 November 2005; published 15 February 2006.

[1] In this paper we present a study on stratospheric intrusion (SI) events recorded at a high mountain station in the Italian northern Apennines. Six years (1998–2003) of surface ozone and beryllium-7 concentration measurements as well as relative humidity values recorded at the GAW Mt. Cimone research station (44°11′N, 10°42′E; 2165 m asl) were analyzed. Moreover, three-dimensional backward trajectories calculated by the FLEXTRA model and potential vorticity values along these trajectories were used. In order to identify SI and evaluate their contribution to the tropospheric ozone at Mt. Cimone, a statistical methodology was developed. This methodology consists of different selection criteria based on observed and modeled stratospheric tracers as well as on tropopause height values recorded by radio soundings. On average, SI effects affected Mt. Cimone for about 36 days/year. The obtained 6-year SI climatology showed a clear seasonal cycle with a winter maximum and a spring-summer minimum. The seasonal cycle was also characterized by an interannual variation. In particular, during winter (autumn), SI frequency could be related to the intensity of the positive (negative) NAO phase. In order to separate direct SI from indirect SI, a restrictive selection criterion was set. This criterion, named Direct Intrusion Criterion (DIC), requested that all the analyzed tracers were characterized by stratospheric values. Direct SI affected Mt. Cimone for about 6 days/year, with frequency peaks in winter and early summer. At Mt. Cimone, SI contribution to background ozone concentrations was largest in winter. On average, an ozone increase of 8% (3%) with respect to the monthly running mean was found during direct (indirect) SI. Finally, the typical variations of stratospheric tracers during SI events were analyzed. The analysis of in situ atmospheric pressure values suggested that direct SI were connected with intense fronts affecting the region, while indirect SI were possibly connected with subsiding structures related with anticyclonic areas.

Citation: Cristofanelli, P., P. Bonasoni, L. Tositti, U. Bonafè, F. Calzolari, F. Evangelisti, S. Sandrini, and A. Stohl (2006), A 6-year analysis of stratospheric intrusions and their influence on ozone at Mt. Cimone (2165 m above sea level), *J. Geophys. Res.*, *111*, D03306, doi:10.1029/2005JD006553.

1. Introduction

[2] Stratosphere-troposphere exchange (STE) influences the chemical composition of both the stratosphere and the troposphere and represents an important aspect of global change [*Butchart and Scaife*, 2001; *Collins et al.*, 2003; *Land and Feichter*, 2003; *Sudo et al.*, 2003]. It is also often associated with severe weather events [*Goering et al.*, 2001]. Many studies have tried to determine the contribution of stratosphere-to-troposphere transport (STT) to tropospheric ozone (O_3), one of the most important gases involved in photochemical reactions [*Crutzen et al.*, 1999; *Volz-Thomas et al.*, 2002]. Even if it is currently thought that the greatest contribution to tropospheric O_3 comes from photochemical production [*Staehelin et al.*, 1994; *Yenger et al.*, 1999], the contribution of STT cannot be neglected [*Roelofs and Lelieveld*, 1997]. Being the precursor of oxidizing substances like OH and NO_3, O_3 is one of the key agents determining the oxidation capacity of the troposphere [*Gauss et al.*, 2003]. Owing to its chemical properties, O_3 is also a dangerous secondary pollutant in the lower troposphere [*Hoek et al.*, 1993; *Kinney*, 1993]. Moreover, there has been great interest in the influence of tropospheric O_3 on climate over the last decades, because it plays a central role in the radiative budget of the atmosphere [*Ramaswamy et al.*, 2001]. For understanding the factors influencing the tropospheric O_3 budget, continuous monitoring of ozone and related variables performed in background conditions (i.e., conditions not directly influenced by anthropogenic activities) still represents a fundamental activity. Besides being very suitable to study tropospheric background conditions [*Wotawa et al.*, 2000], mountain

[1]National Research Council, Institute of Atmosphere and Climate Sciences, Bologna, Italy.
[2]Environmental Radiochemistry Laboratory, Chemistry Department, Bologna University, Bologna, Italy.
[3]Norsk Institutt for Luftforskning, Kjeller, Norway.

0148-0227/06/2005JD006553$09.00

Table 1. Radiosounding Data Used to Determine Tropopause Deformations Over Mt. Cimone Area

Station	ID	Location	Highest Sounding Frequency	Data Availability, %
Ajaccio	AJA	41.92N, 8.80E, 5 m asl	2/day	69
S.Pietro Capofiume	CAP	44.65N, 11.62E; 38 m asl	2/day	55
Milano-Linate	MIL	45.43N, 9.28E; 103 m asl	4/day	81
Udine	UDI	46.03N, 13.18E, 92 m asl	4/day	79
Lyon	LYO	45.73N, 5.08E, 7 m asl	4/day	61
Payerne	PAY	46.82N, 6.95E, 490 m asl	2/day	67
München	MUN	48.25N, 11.58E, 484 m asl	2/day	67
Hohenpeisssenberg	HOH	47.80N, 11.02E, 986 m asl	1/day	17

peak stations are also appropriate locations to investigate a specific aspect of STT: stratospheric intrusion (SI) events, i.e., the downward transport of stratospheric air masses relatively deep into the troposphere. Nevertheless, caution should be taken in generalizing results achieved by identifying SI at a single mountain peak top.

[3] The most important phenomena promoting SI are tropopause folds [*Reed*, 1955] and cutoff lows [*Vaughan and Price*, 1989] at the upper levels and fronts or surface high-pressure systems at the surface [*Davies and Schuepbach*, 1994]. The downward motion of stratospheric air in the lower troposphere can occur in a direct or indirect way [*Zanis et al.*, 1999]. While in the case of direct SI stratospheric air maintains for a large part its stratospheric properties as it reaches the lower troposphere by rapid vertical transport, indirect SI reach the lower troposphere after a sequence of transport steps, giving it a greater chance to mix with tropospheric air [*Eisele et al.*, 1999]. Usually, because of mixing processes acting on small and intermediate ($\sim$100 km) scales, stratospheric air masses quickly lose their original properties [*Appenzeller and Davies*, 1992], making difficult the identification of originally stratospheric air masses at low altitudes. Therefore high mountain stations are privileged platform for SI observations, but the capability to detect SI relies on the continuous monitoring of specific atmospheric tracers. The frequency at which SI are detected in measurement records is sensitive to the criteria used to identify these events [*Scheel et al.*, 1999; *Stohl et al.*, 2000]. However, numerical simulations of SI still need further improvements to correctly capture such events [*Cristofanelli et al.*, 2003; *Meloen et al.*, 2003]. Thus the analysis of SI still relies heavily on measurements.

[4] In this paper, we study SI that affected Mt. Cimone (44°11′N, 10°42′E; 2165 m asl) in the period 1998–2003. In the next section, the measurement data and the model products used to investigate the SI are described. In section 3, a brief survey about the principal stratospheric tracers used in this paper is presented. Then, the methodology used to identify SI is presented and applied to determine the SI frequency at Mt. Cimone. In section 4, the influence of SI on surface ozone concentrations recorded at the measurement site is assessed. In section 5, we describe the typical behavior of ozone and stratospheric tracers during SI at Mt. Cimone. Finally, conclusions are drawn.

2. Site and Measurements

[5] Mt. Cimone is the highest peak of the Italian northern Apennines. Large industrialized and urban areas are far away from the measurement site, thus the Mt. Cimone measurements of atmospheric compounds and meteorological parameters can be considered well representative of the southern European free troposphere [*Bonasoni et al.*, 2000a; *Fischer et al.*, 2003]. The study of SI represents one of the activities conducted at this research station and therefore parameters that are helpful to identify SI are continuously monitored. The ''Ottavio Vittori'' research station is part of the Global Atmosphere Watch programme (GAW) of the World Meteorological Organization (WMO) and tropospheric O_3 measurements have been carried out continuously since 1996 by using a UV-photometric analyzer (Dasibi 1108). The accuracy and the quality of measurements (time sampling: 1-min, accuracy and precision: ±2 ppb) are guaranteed within the GAW requirements.

[6] Continuous monitoring of ^{7}Be concentrations at Mt. Cimone started in 1998, after isolated measurements were performed in 1996 and 1997. The sampling activity has been carried out with a time resolution of about 48 hours by using a Thermo-Environmental PM10 High-Volume sampler (flow rate: 1.13 m^3 min^{-1}). ^{7}Be concentrations are determined on the sampled glass fiber filters by nondestructive high-resolution γ-spectroscopy at 478 keV with HPGe detectors at the Laboratory of Environmental Radiochemistry of the Bologna University. In addition to the usual procedures to test laboratory performances, accuracy and precision of ^{7}Be measurements were evaluated within an intercomparison exercise which involved several European research groups [*Tositti et al.*, 2004].

[7] In order to determine the origin of air masses reaching Mt. Cimone, 6-day three-dimensional backward trajectories calculated by the FLEXTRA model [*Stohl et al.*, 1995] have been analyzed. Trajectory calculations, with an horizontal resolution of 1° × 1°, are based on meteorological analysis and 3-hour forecast fields produced by the numerical weather prediction model of the European Centre for Medium Range Weather Forecasts (ECMWF). For each day, eight trajectories are available with their positions recorded every 3 hours. For every point along the trajectory the model provides the air mass position (geographic location and altitude) as well as potential temperature and potential vorticity.

[8] In order to determine tropopause heights (TPH) over the Mt. Cimone region, data obtained at eight WMO radiosounding stations located North and South of Alps have been analyzed. As sounding data were available with different time resolution and at different times (Table 1), 24-hour means calculated for each station have been used.

3. Identification of SI at Mt. Cimone

3.1. Stratospheric Tracers

[9] Experimental studies of SI are usually based on the analysis of the temporal variations of specific stratospheric

Table 2. General Statistic of the Different Atmospheric Compounds and Parameters Analyzed

Parameter	Number of Data	Average	Median	25th Percentile	75th Percentile	Max	Min	Dev. Std.
Daily O_3, ppbv	2088	54	53	47	61	100	24	10
RH_{Min}, %	2189	57	56	37	79	100	0	26
PV, pvu	2132	1.33	1.12	0.90	1.43	8.26	0.26	0.80
^{7}Be, mBq m^{-3}	1946	4.6	4.5	2.7	6.2	15.7	0.2	2.5

tracers [*Elbern et al.*, 1997; *Stohl et al.*, 2000; *Scheel*, 2002; *Allen et al.*, 2003; *Zanis et al.*, 2003]. Typically, stratospheric tracers are either chemical compounds or physical quantities that have strong differences between the stratosphere and the troposphere. In this paper, we considered as stratospheric tracers a set of parameters that has widely been used to identify SI (see references in the following paragraphs): relative humidity, potential vorticity and ^{7}Be. Moreover, as SI can be connected with intense tropopause deformation [*Buzzi et al.*, 1985; *Schuepbach et al.*, 1999], TPH over the Mt. Cimone region was also considered. Because our study focuses on the evaluation of SI contribution to tropospheric O_3 concentration, O_3 was not included in the tracer analysis in order to avoid a potential bias. Basic statistics on stratospheric tracers and O_3 at Mt. Cimone are presented in Table 2, and time series of O_3 is shown in Figure 1a. In order to develop a methodology to detect SI, for each tracer we defined a threshold value above which an air mass is considered to have a stratospheric character. The availability of data analyzed is reported in Table 3, while in the following paragraphs a brief survey on the different stratospheric tracers analyzed in our work is given, together with the threshold values defined to select SI at Mt. Cimone.

3.1.1. Relative Humidity (RH)

[10] Besides having high ozone concentrations, air masses originating in the stratosphere are characterized by low water vapor contents [*Bithell et al.*, 1999]. Thus low humidity levels can indicate stratospheric air in the troposphere. RH can be considered the best humidity measure to detect SI. In fact, since stratospheric air mixes with tropospheric air masses during its descent, considering the specific humidity (which is highly variable with the seasons in tropospheric air) can lead to an artificial bias in the evaluation of seasonal SI frequency [*Stohl et al.*, 2000].

[11] The analysis of several cases [*Bonasoni et al.*, 1999; *Bonasoni et al.*, 2000b] suggested to adopt a RH threshold of 40% to identify SI at Mt. Cimone. This threshold value, already applied by *Scheel et al.* [1999] and *Stohl et al.* [2000] to detect SI at other high mountain stations, was not an arbitrary choice. In fact, the analysis of t-Test value for the significance of the difference between the means of daily ozone residual (i.e., the difference between daily ozone values and the corresponding monthly running mean centered on the respective day), when sorted according to a separation value of daily RH minimum, presented two distinct classes above and below the RH value of about 40% (here not shown). This suggests that transport processes of air masses characterized by RH above and below this value are systematically different, thus influencing ozone concentration at Mt. Cimone. Assuming that SI can be involved in the appearance of the lower RH mode is thus a reasonable hypothesis.

3.1.2. Potential Vorticity (PV)

[12] In absence of diabatic heating or frictional forces, potential vorticity P_θ is a conserved quantity [*Ertel*, 1942]. In its isentropic form P_θ is defined by:

$$P_\theta = -g\ \partial\theta/\partial p(\xi_\theta + f)$$

where g denotes the gravity acceleration, θ the potential temperature, p the pressure, ξ_θ the component of the curl of wind vector normal to an isentropic surface, and f the Coriolis parameter. In different studies, potential vorticity (hereinafter, PV) has been used to trace stratospheric air in the troposphere [*Beekmann et al.*, 1994; *Poulida et al.*, 1996]. In fact, the ozone layer in the stratosphere produces a highly stable stratification (i.e., a strong positive vertical gradient of potential temperature), such that the PV is several orders of magnitude greater than in troposphere [*Beekmann et al.*, 1994]. In fact, in the atmosphere above 350 hPa, PV rapidly increases with

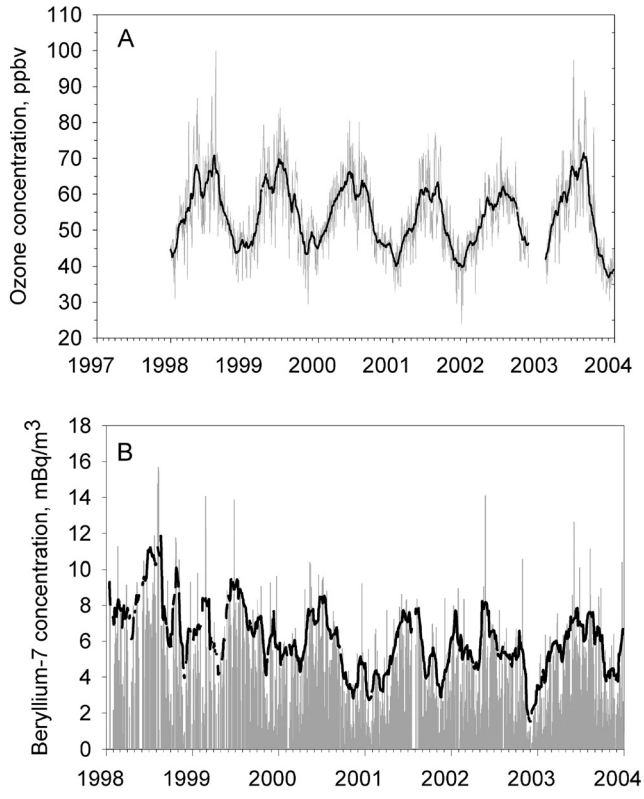

Figure 1. (a) Behavior of daily O_3 at Mt. Cimone during the period of study. The continuous line represents the monthly running mean. (b) ^{7}Be behavior at Mt. Cimone during the period of study. The continuous line represents the running threshold t_D^{Be} applied to the Mt. Cimone data.

Table 3. Data Availability for the Period 1998–2003 at Mt. Cimone

Year	Daily O_3, %	RH_{Min}, %	PV, %	^{7}Be, %
1998	100	100	98	72
1999	99	100	95	80
2000	100	100	100	96
2001	99	100	100	93
2002	82	99	100	94
2003	91	100	91	98

altitude, reaching typical values from 1.0 pvu [*Danielsen*, 1968] to 3.5 pvu [*Hoerling et al.*, 1991] at tropopause level, where 1 pvu = 1×10^{-6} m^2 K kg^{-1} s^{-1}. In this study we considered as a signature of stratospheric air at Mt. Cimone, the presence of air masses characterized by PV values greater than 1.6 pvu along the trajectory path. The choice of the rather low value of 1.6 pvu as a threshold for stratospheric air is justified by the fact that the trajectories may not go back all the way deeply into the stratosphere because of their limited length and also because of possible trajectory errors. High PV values can also be generated by diabatic processes in the lower troposphere (e.g., strong nighttime cooling at the surface or diabatic heating due to the condensation of water vapor). In order to avoid a misidentification of stratospheric air masses, we used the 1.6 pvu threshold only at altitudes higher than 5000 m [*Olsen et al.*, 2000].

3.1.3. Beryllium-7 (^{7}Be)

[13] High concentrations of ^{7}Be are indicative for SI [*Reiter et al.*, 1983], because this radionuclide is produced in the stratosphere and upper troposphere by nuclear reaction between cosmic rays (neutrons and protons) and the nuclei of the most abundant atmospheric gases (nitrogen and oxygen) [*Lal and Peters*, 1967]. Different studies have emphasized the importance of the cosmogenic radionuclide ^{7}Be ($t_{1/2}$ = 53 days) as a tracer of stratospheric air in the troposphere [*Zanis et al.*, 2003; *Allen et al.*, 2003]. However, in the troposphere ^{7}Be concentrations are largely determined by the fate of its carrier aerosol, which is affected strongly by wet/dry scavenging [*Gerasopoulos et al.*, 2001; *Zanis et al.*, 1999]. Moreover, because one third of ^{7}Be is produced in the upper troposphere [*Dutkiewicz and Husain*, 1985; *Koch and Mann*, 1996; *Koch et al.*, 1996], it is not possible to consider ^{7}Be as an unambiguous stratospheric tracer [*Zanis et al.*, 1999; *Stohl et al.*, 2000]. In previous publications [*Slàdkovic and Munzert*, 1990; *Stohl et al.*, 2000], a threshold value of 8 mBq/m^3 was suggested to identify stratospheric air masses at the mountain station Zugspitze (2962 m asl). However, it may not apply automatically also to other high-elevation sites, i.e., Mt. Cimone. In addition, since ^{7}Be shows strong seasonal and interannual variability (Figure 1b) driven by different controlling factors such as solar activity, circulation patterns and meteorology [*Feely et al.*, 1989; *Arimoto et al.*, 1999; *Gerasopoulos et al.*, 2003; *Lee et al.*, 2004; *Hernández et al.*, 2005], using a fixed threshold of 8 mBq/m^3 to identify SI at Mt. Cimone could be inappropriate. For these reasons, the selection of days influenced by SI is based on one of the following criteria: (1) Daily ^{7}Be value is greater than 8 mBq/m^3; (2) daily ^{7}Be value is greater than a running threshold (t_D^{Be}) dependent on both the ^{7}Be monthly running mean and the ^{7}Be residual:

$$t_D^{Be} = \overline{^7Be}_D + \frac{\sum_{D=1,N} \left| \overline{^7Be}_D - {}^7Be_D \right|}{N}$$

where, $\overline{^7Be}_D$ represents the ^{7}Be monthly running mean calculated for each day of the sampling month, ^7Be_D is the ^{7}Be concentration recorded at the Dth sampling and N the number of samplings carried out during the month. The behavior of t_D^{Be} is shown in Figure 1b. Previous studies [*James et al.*, 2003; *Sprenger and Wernli*, 2003] demonstrated that atmospheric variability patterns (e.g., the North Atlantic Oscillation) can influence year-to-year variability of STT. In order to avoid that our ^{7}Be selection could mask interannual variability in the SI, the fixed threshold value of 8 mBq/m^3 has been also included (criterion 1).

3.1.4. Tropopause Height (TPH)

[14] As reported by *Davies and Schuepbach* [1994], SI can occur during tropopause folding events, associated with a wide range of phenomena like upper level frontogenesis, rapid surface cyclogenesis, pronounced upper troughs and cutoff lows. During these phenomena, a tropopause descent is often associated with the injection of stratospheric air into troposphere [*Buzzi et al.*, 1985; *Bonasoni et al.*, 1999; *Elbern et al.*, 1997; *Schuepbach et al.*, 1999]. In order to point out tropopause deformation over Mt. Cimone area, TPH values deduced from radio soundings carried out at eight locations North and South of the alpine region have been analyzed (Table 1). In accord with WMO operational definition, in this work, TPH has been defined as the lowest pressure level at which the lapse rate temperature decreases to 2° K/km or less, and the average lapse rate from this level to any level within the next higher 2 km does not exceed 2° K/km [*U.S. Department of Commerce*, 1976].

3.2. Screening Methodology and Direct Intrusion Criterion (DIC) Definition

[15] In order to identify SI at Mt. Cimone and evaluate their influence on background O_3 concentration in the period 1998–2003, we classified a day as being influenced by a SI if (1) the daily minimum RH is lower than 40%, (2) one of the eight daily FLEXTRA back trajectories has a PV value above 1.6 pvu at altitude higher than 5000 m

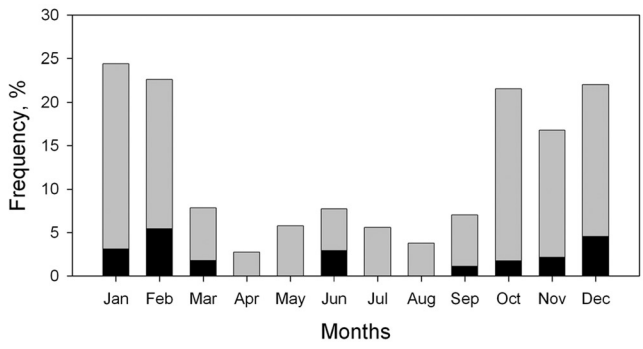

Figure 2. Seasonal variation of the frequency of selected days. Shaded area represents "indirect intrusions," and solid area represents "direct intrusions."

Table 4. Percentage of Days Selected by the Different Criteria Applied During the Period of Study[a]

Criteria	1998, %	1999, %	2000, %	2001, %	2002, %	2003, %	Whole Period, %
RH	31.2	20.0	27.9	22.8	23.9	26.0	25.3
PV	18.1	19.3	14.0	13.3	9.9	12.2	14.3
^{7}Be	21.5	20.4	19.7	21.0	20.1	21.1	20.6
RH-PV	5.0	5.8	4.6	6.8	2.5	3.6	4.7
RH-^{7}Be (TPH)	9.2 (8.8)	7.3 (7.3)	11.4 (8.3)	9.5 (6.8)	9.2 (7.4)	11.8 (5.9)	9.8 (7.4)
PV-^{7}Be	3.5	3.6	4.3	4.1	4.6	3.6	4.0
RH-PV-^{7}Be	1.9	2.2	1.7	1.8	2.1	1.3	1.8

[a]Referring to RH-^{7}Be criterion, the values in parenthesis show the number of days selected by using the additional TPH filter.

asl, or (3) ^{7}Be concentration is higher than 8 mBq/m^3 or higher than the variable threshold t_D^{Be}. Among the 1812 days analyzed, 25.3% fulfilled the RH condition, 14.3% the PV condition and 20.6% the Be^{7} condition (Table 4). Because of missing data and a few gaps in the back trajectory data set, simultaneous data for all parameters were available for 83% of the studied period.

3.2.1. Selection of Days Influenced by SI

[16] In order to select the periods influenced by SI, we considered the days when at least two of the considered tracers showed ''stratospheric'' values (Table 4). In this way, a first selection of days with O_3 concentrations possibly influenced by SI could be made: 4.7% of analyzed days satisfied the combined RH-PV criterion, 9.8% satisfied the RH-^{7}Be criterion and 4.0% satisfied the PV-^{7}Be criterion. The RH-^{7}Be selection was the least restrictive criterion, resulting in the highest frequency of SI at Mt. Cimone. However, as previously reported, ^{7}Be and RH are often considered not unambiguous SI tracers (see section 3.1). In fact, especially during warm months, relatively high ^{7}Be and low RH can be found in the lower troposphere even when the meteorological situation and circulation patterns does not suggest an occurrence of a SI. This is mainly due to the efficient vertical mixing of the atmosphere in summer that enhances the downward transport of drier air masses from the upper troposphere [*Feely et al.*, 1989; *Gerasopoulos et al.*, 2001, 2003]. Therefore SI frequency can be overestimated if only RH and ^{7}Be are used as stratospheric tracers. With the aim to prevent such wrong detections, during the nonwinter period (March to September as defined for the Mediterranean region by *Trigo et al.* [2002]) we considered TPH as an additional stratospheric tracer. Previous studies [*Zanis et al.*, 1999; *Gerasopoulos et al.*, 2001] showed that in the lower troposphere TPH is positively correlated with ^{7}Be: during high tropopause conditions, high ^{7}Be concentrations can be transported from upper troposphere. Thus we can suppose that high ^{7}Be and low RH conditions recorded during tropopause lowering could be linked with SI occurrence. The detection of low TPH has been based on the analysis of the daily TPH standardized anomaly recorded at each station. A day has been considered as affected by tropopause deformation if, during a 3-day interval ending at the analyzed day, at least 50% of the considered stations experienced significantly (at the 95% confidence level) low TPH with respect to the monthly mean value. By applying this algorithm, among the days selected by the RH-^{7}Be criterion, we retained only 134 days (7.4% of the whole data set).

[17] In order to evaluate the covariance between the number of SI selected by the different selection criteria, we provided three 2 × 2 contingency tables for the detection of SI (Table 5). For each one of the three contingency tables, we compared the skill of two selection criteria (i.e., RH-^{7}Be versus RH-PV; RH-^{7}Be versus PV-^{7}Be and RH-PV versus PV-^{7}Be) in detecting (or no detecting) SI. With this aim, for each criterion we distinguished between the days selected as SI influenced and those not selected as SI influenced (No SI). Then, the percentage (score) of these days identified as SI or No SI also by the remaining tracers was calculated. This analysis showed that the highest number of simultaneous SI detection (2.3% of the data set) has been carried out by RH-PV and PV-^{7}Be criteria. On the other hand, the score in detecting No SI appeared high for all the selection criteria, showing that they work well in correctly identifying (and thus excluding) No SI (Table 5). With the purpose to assess the statistical significance of the agreement between the different criteria in selecting SI, we calculated a skill score index between each pair of selection criteria. For each pair of criteria, we calculated the Odds Ratio Skill Score (ORSS) [*Thornes and Stephenson*, 2001] which is given by:

$$ORSS = \frac{A \times B - B \times C}{A \times D + B \times C}$$

where, for each pair of criteria, A represents the number of days selected as SI by both criteria; D represents the number of days selected as No SI by both criteria; B represents the number of days selected as SI by the first criterion but as No SI by the second criterion and C represents the number of days selected as No SI by the first criterion but as SI by the second criterion. This ORSS is an index usually applied to judge the weather forecast quality by comparing the odds of making a hit (good forecast) with those of making a false alarm (bad forecast). It varies between +1 and −1 where a value of +1 represents a perfect skill, a value of zero represents no skill and negative numbers imply that the forecast were opposite to what was observed. It is also possible to assess the statistical significance of this verification index. Particularly, the analysis of the ORSS based on data reported in Table 5 showed that the agreement between the different criteria in selecting SI was not due to chance (at the 99.9% confidence level).

[18] In total, by considering all days identified by at least one of the criteria pairs, 213 days were selected as ''stratospheric influenced'' during the period of study, which represents 11.7% of the analyzed days: for at least 36 day/year air masses containing stratospheric ''fingerprints'' could reach Mt. Cimone in the period 1998–2003. These results pointed out that SI could play an important role in determining background O_3 concentrations at this baseline station. The days selected by a pair of tracers (RH-^{7}Be or

Table 5. Contingency Tables for the Detection of SI Events as Selected by the Different Criteria Applied[a]

	RH-^{7}Be		
RH-PV	SI	No SI	ORSS
SI	A = 1.8%	B = 2.9%	
No Si	C = 5.6%	D = 89.7%	
ORSS			0.82 (0.45)
	RH-^{7}Be		
PV-^{7}Be	SI	No SI	ORSS
SI	A = 1.8%	B = 2.1%	
No SI	C = 5.6%	D = 90.5%	
ORSS			0.87 (0.45)
	RH-PV		
PV-^{7}Be	SI	No SI	ORSS
SI	A = 2.3%	B = 1.6%	
No SI	C = 2.3%	D = 93.7%	
ORSS			0.97 (0.45)

[a]For each criterion the percentage (in respect with the whole data set) of detection (SI) or no detection (No SI) of SI are compared with the results provided by other criteria. Capital letters denote the following: A, percentage of days selected as SI by both criteria; D, percentage of days selected as No SI by both criteria; B, percentage of days selected as SI by the first criterion but as No SI by the second criterion; C, percentage of days selected as No SI by the first criterion but as SI by the second criterion. For each pair of criteria the calculated ORSS is reported together with the minimum value of the ORSS (in parentheses) required in order to have real skills at the 99.9% confidence level [*Thornes and Stephenson,* 2001].

RH-PV or PV-^{7}Be) and thus characterized by a greater loss of stratospheric properties, are indicated as indirect SI hereinafter. Finally, with the aim to define a criterion able to select only direct SI (characterized by stratospheric air masses that largely conserved their chemical-physical properties after intrusion in troposphere), we selected those days during which all the stratospheric tracers exceeded their threshold values (Direct Intrusion Criterion (DIC)). The simultaneous analysis of the three tracers (RH, PV and ^{7}Be) plus the TPH led to the identification of 33 days (6 days/year), which represents 1.8% of the study period (Table 4).

3.2.2. Analysis of SI Frequency Variability

[19] In order to define the variability of direct and indirect SI, the month-to-month variation of averaged SI frequency was calculated (Figure 2). The monthly SI frequency showed a maximum from December to February, a secondary maximum in autumn (October) and a minimum from spring to summer. In particular, in April (August) the number of detected SI amounts to about 14% (16%) of the January peak value. In contrast with indirect SI (shaded area in Figure 2), the direct SI seasonal cycle (solid area in Figure 2) was characterized by the absence of a clear maximum, with high values in winter (December–February) and early summer (June). However, the number of direct SI was so low that this seasonal pattern may not be robust.

[20] With the purpose to analyze the year-to-year variability of SI frequency, we calculated the occurrence of selected days (indirect + direct SI) for each meteorological season: winter (December–February), spring (March–May), summer (June–August) and autumn (September–November). We calculated the SI seasonal occurrence as the ratio between the number of selected days and the number of analyzed days for each season (Figure 3). At Mt. Cimone, the SI frequency showed a clear seasonal cycle with a maximum in winter and a minimum in spring-summer with average peak-to-peak ratio amplitude of 0.18. Nevertheless, the obtained seasonal cycle showed also a year-to-year variability. For instance, the winter maximum in 2001 was about 40% (60%) smaller than in 2000 (2002). Part of this interannual variability could be explained considering the seasonal activity of the NAO, one of the most prominent and recurrent patterns of atmospheric circulation variability in the North Atlantic basin [*Defant*, 1924; *Wallace and Gutzler*, 1981; *Hurrell et al.*, 2003]. Previous studies [*Sprenger and Wernli*, 2003; *James et al.*, 2003] suggested that the NAO can affect the geographical exchange patterns and the frequency of deep STT over the Atlantic and Europe during winter, when the NAO exerts a strong control on the climate of the northern Hemisphere [*Marshall et al.*, 2001]. We investigated possible differences in the SI frequency at Mt. Cimone related to the NAO index (NAOI). For this purpose, for each season during the period 1998–2003, we considered the seasonal NAOI (as defined by *Jones et al.* [1997]). With the aim to increase the analysis reliability, in this framework only those seasons with data availability greater than 70% have been considered. A possible relationship has been pointed out between the SI frequency in the winter (autumn) and the positive (negative) phase of the NAO in the same season. In fact, winters with the highest SI frequencies (i.e., 1999, 2000 and 2002; bold characters in Table 6) were also characterized by the strongest positive NAO phases, whereas autumns with the highest SI frequen-

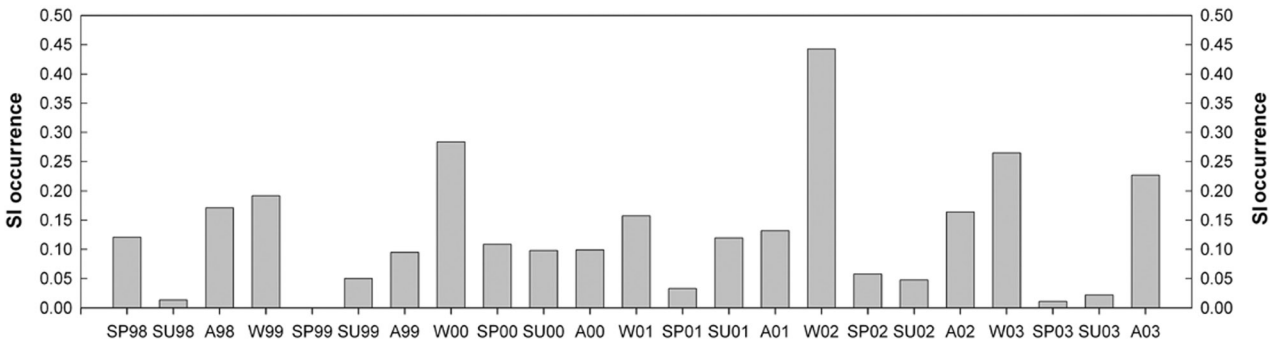

Figure 3. Seasonal SI occurrence (expressed as the ratio selected/analyzed days) of selected days.

Table 6. SI Frequency Recorded at Mt. Cimone, the Seasonal NAOI as Well as the Highest (Lowest) Monthly NAOI for Winter (Autumn) From 1998 to 2003[a]

	Winter			Autumn		
Year	SI Frequency	NAOI	Highest NAOI	SI Frequency	NAOI	Lowest NAOI
1998	...	...	...	0.17	−0.34	−3.48
1999	**0.19**	**+1.55**	**+1.95**	0.09	−0.30	0.69
2000	**0.28**	**+2.28**	**+4.37**	0.10	0.31	1.10
2001	0.16	−0.44	+0.07	**0.13**	**−0.98**	**−3.83**
2002	**0.44**	**+1.02**	**+3.01**	**0.16**	**−1.78**	**−3.58**
2003	...	...	...	**0.23**	**−1.01**	**−3.68**

[a]Only seasons with at least the 70% data availability have been considered.

cies (i.e., 2001, 2002 and 2003; bold characters in Table 6) were characterized by strong negative NAOI. It could be argued that for winter 2002 the highest SI frequency (0.44) was not related with the strongest positive NAO regime, and that for autumn 1998 a quite elevated SI frequency (0.17) was recorded with a weak seasonal NAO regime (−0.34). For this reasons, we looked more in detail at the NAO behavior considering the largest positive (for the winters) and the greatest negative (for the autumns) monthly NAOI. As reported in Table 6, it appeared that all the winters (autumns) with high SI frequency have been also characterized by the presence of at least one month with a very strong positive (negative) NAOI (see for example, autumn 1998 and winter 2002). Thus, even if a 6-year analysis represents a too short period to allow conclusive results, nevertheless it could suggest the existence of a link between the occurrence of SI at Mt. Cimone and the NAO during winter and autumn.

4. Influence of SI on Surface O_3 Concentration Recorded at Mt. Cimone

[21] The surface O_3 concentration recorded at Mt. Cimone during the period of study (yearly mean value: 54 ± 10 ppbv) is characterized by a seasonal cycle with an average monthly minimum of about 40 ppbv in winter and a maximum of about 65 ppbv in summer (Figure 1a). No clear daily O_3 cycle is observed at Mt. Cimone, except for some periods during the warm season when a small reverse diurnal variation can be caused by the local upslope winds [*Bonasoni et al.*, 2000a].

[22] In order to evaluate the influence of SI on surface ozone concentration at Mt Cimone, we calculated the daily ozone variation (ΔO_3) recorded during SI with respect to the monthly running mean. Even if negative ΔO_3 values have been recorded for 32% of the selected days, a significant (at the 95% confidence level) average increase of daily ozone concentration (ΔO_3: 3%) was recorded for indirect SI. For direct SI, ΔO_3 was almost always positive, with an average ozone increase of 8%. This is best seen in Figure 4, where the boxes and whiskers denote the 5th, 25th, 50th, 75th, 90th percentiles, while the bold lines represent the arithmetic means for ΔO_3 during the different seasons. The average seasonal contribution for direct SI shows a seasonal cycle with high O_3 contributions in winter (mean value: 9%) and the lowest in spring (5%). However, these latter data should be considered with caution because of the small number of direct SI recorded during this season. Concerning indirect SI, the ΔO_3 seasonal variation showed the highest O_3 contributions in winter (mean value: 4%) and the lowest in summer (<1%). This analysis showed that only a small fraction of direct SI (3 out 33) has been characterized by negative ΔO_3 (during winter all direct SI caused positive ΔO_3), while a larger fraction of indirect SI (particularly during warm months) has been accompanied by negative ΔO_3. However, 91% of the SI with negative daily ΔO_3 have been characterized by significant increases of the hourly O_3 concentrations with respect to the monthly running mean (average maximum increase: 8%). Thus we can suppose that these days could be influenced by actual O_3 increases, but of a too short duration (only a few hours) to significantly affect the daily means. In fact, considering an interval of 11 days around the selected SI, it has been pointed out that 88% of the events characterized by $\Delta O_3 < 0$ has been preceded (50%) or followed (38%) by periods with significantly high O_3 values. The latter situation can be related to the role played by SI on triggering photochemical O_3 formation by providing an extra source of hydroxyl (OH) radicals [*Stohl et al.*, 2000; *Feldmann et al.*, 1999]. On the other hand, the former situation can be related to the possibility that, especially during warm months, the lower troposphere over southern Europe is characterized by elevated photochemical O_3 production and accumulation that might limit the importance of stratospheric inputs.

5. Analysis of SI Events at Mt. Cimone

[23] In this paragraph, we will provide a description of the typical variations of daily O_3 and stratospheric tracers during SI events by applying the methodology presented by *Elbern et al.* [1997]. An interval of 11 days around the selected SI was considered. Thus, for each day, the average

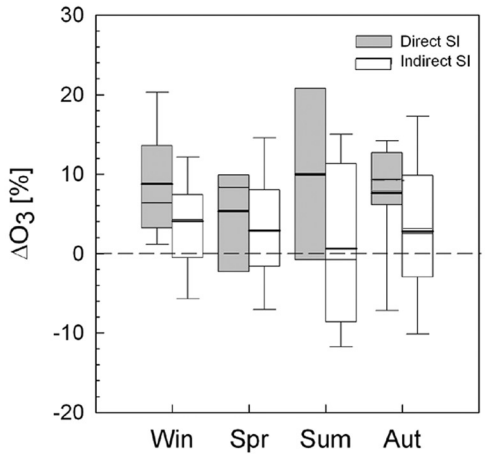

Figure 4. Box-and-whiskers plot of daily O_3 variations (ΔO_3) during direct (shaded) and indirect (open) SI at Mt. Cimone for the different seasons. Seasons are defined as following: winter (December–February), spring (March–May), summer (June–August), and autumn (September–November). The box and whiskers denote the 5th, 25th, 50th, 75th and 95th percentile, while the bold lines denote the arithmetic means.

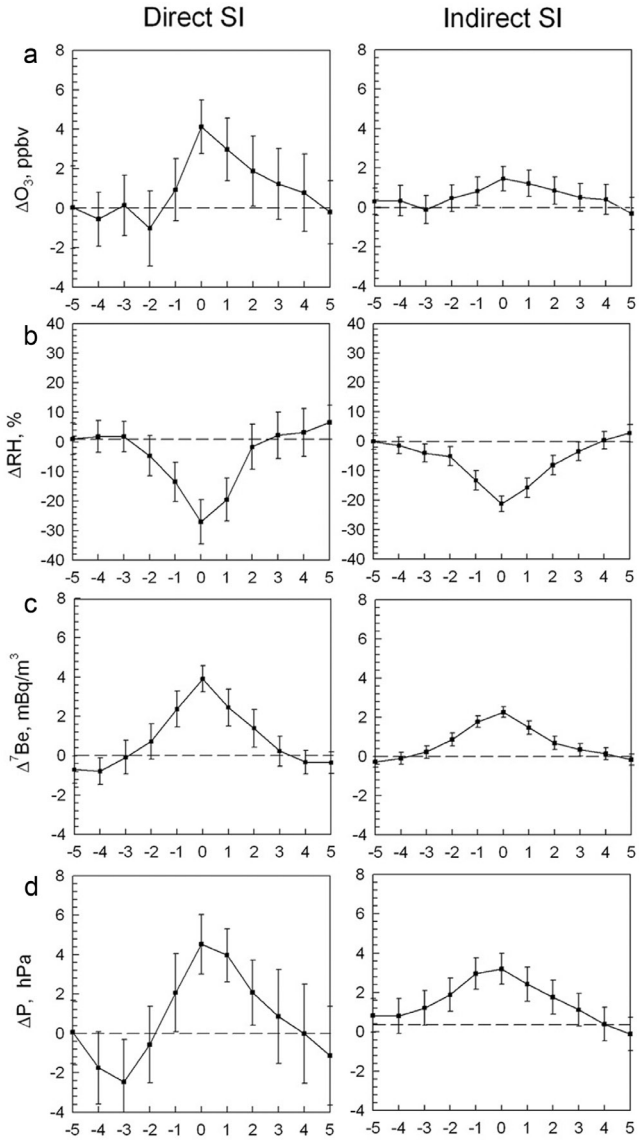

Figure 5. Behavior analysis for (a) daily ozone concentration, (b) relative humidity, (c) ^{7}Be concentration, and (d) atmospheric pressure in a 11-day interval centered on "direct" (left column) and "indirect" (right column) SI events (day zero). Dotted line represents the averaged value on the monthly interval centered in the selected event. The vertical bars represent the 95% confidence level.

deviation $C^{x}(i)$ from the monthly running mean was calculated for O_3 and stratospheric tracers:

$$C^{X}(i) = \frac{1}{N}\sum_{k=1}^{N}\left(C_k^{X}(i) - \overline{C^{X}}\right), \quad i = -5, \ldots, 0, \ldots, 5,$$

where $C^{x}{}_{k}(i)$ represents the daily values of X (RH, ^{7}Be or O_3) recorded at the ith day from the kth selected SI ("indirect" or "direct"), $\overline{C^{x}}$ represents the monthly running mean and N the number of selected days. Moreover, the median daily atmospheric surface pressure values were also analyzed to better describe the typical SI at Mt. Cimone.

[24] The results of this analysis show that on average direct SI events (Figure 5, left column) were characterized by a significant (at the 95% confidence level) sharp O_3 increase (4.1 ppbv), with a simultaneous large decrease in RH (−27%) and increases in ^{7}Be and atmospheric pressure (3.9 mBq/m^3 and 4.5 hPa, respectively).

[25] Concerning indirect SI events (Figure 5, right column), a smaller broad O_3 peak (1.5 ppbv) occurred simultaneously with average RH decrease (−21%) as well as ^{7}Be (2.3 mBq/m^3) and atmospheric pressure (3.2 hPa) increases. While direct SI were characterized by a large pressure increase ($\Delta P \approx 7.0$ hPa/72 hours, see Figure 5, left column) which could be connected with front passages, indirect SI showed a smaller pressure increase ($\Delta P \approx 2.0$ hPa/72 hours, see Figure 5, right column). This suggested that during indirect SI, the main stratospheric input at Mt. Cimone is probably related to subsiding structures following the primary stratospheric input [*Eisele et al.*, 1999].

[26] Finally, assuming that simultaneous significant variations of O_3 and stratospheric tracers from their background values (see vertical bars in Figure 5) can be indicative for the influence of stratospheric air at the measurement site, the average time length has been estimated to be 2 days for direct SI and 4 days for indirect SI.

6. Discussion and Conclusions

[27] In this paper, a 6-year study (1998–2003) of stratospheric intrusion (SI) events recorded at Mt. Cimone is presented. Particular attention has been devoted to evaluate the contribution of SI on surface ozone concentrations monitored at this GAW station sited in the northern Mediterranean basin and considered representative of south European continental free troposphere. This investigation represents the first attempt to define a systematic analysis of SI in the area south of the Alps, a region well known to be particularly affected by this type of phenomena [*Buzzi et al.*, 1985; *Davies and Schuepbach*, 1994]. Obviously, the identification of SI at this mountain station may not be directly related to quantify large-scale O_3 transfer from the stratosphere to the troposphere.

[28] In order to identify the days influenced by SI, we applied a methodology based on the analysis of stratospheric air mass tracers: ^{7}Be concentrations and RH values continuously monitored at the station, PV values along air mass back trajectories and TPH as deducted by radiosounding activities. After having defined for each tracer threshold values for the possible identification of stratospheric air masses at the measurement site, we applied different combined selection criteria to identify SI at Mt. Cimone. Our analysis suggested that stratospheric air masses reach the measurement site for a significant number of days/year (36). Considering that SI frequencies at other European high mountain stations range from 5% to 14% [*Elbern et al.*, 1997; *Scheel et al.*, 1999; *Stohl et al.*, 2000], our SI frequency (11.7%) appears to be relatively high. The reason for this relies on the fact that these studies required O_3 concentrations to increase significantly during an intrusion day. If in our climatology we had imposed a $\Delta O_3 > 0$ during SI we would have obtained an average SI frequency of 8.3%.

This value would have decreased to 3.2% if we had imposed an O_3 increase of 10% above the monthly running mean. However, in our opinion, to determine a correct SI climatology one cannot rule out the possibility that during SI O_3 can also decrease in respect to background concentrations. In fact, during the last century, the increase of O_3 and precursor emissions due to anthropogenic activities lead to a significant rise of background O_3 levels recorded in the lower troposphere [*Staehelin et al.*, 1994] and, as shown in this work, during specific conditions O_3 concentrations during SI events should be lower than those recorded under the influence of photochemical production episodes.

[29] The adopted screening methodology allows us to demonstrate that the seasonal cycle of SI was characterized by a clear annual variation. In agreement with other experimental and numerical studies carried out in the midlatitudes of the northern Hemisphere [*Elbern et al.*, 1997; *James et al.*, 2003; *Sprenger and Wernli*, 2003], at Mt. Cimone the frequency of SI showed a winter maximum and a spring-summer minimum. A possible relationship between SI frequency at Mt. Cimone and NAO index has been evidenced during winter and autumn, suggesting a connection between SI in the Mediterranean area and the North Atlantic storm track and anticyclones position and intensity.

[30] In order to identify direct SI which reach the lower troposphere by rapid vertical transport maintaining stratospheric fingerprints in the troposphere, we considered a very restrictive criterion named ''DIC.'' This criterion imposed that all the analyzed tracers had ''stratospheric values.'' These direct SI, showed very different characteristics in respect to indirect SI (i.e., air masses having greater mixing with tropospheric air masses and selected by other criteria). On average, direct SI (mean time length: 2 days) affected Mt. Cimone for 6 days/year, with frequency peaks during winter and early summer. Particularly, the high efficiency of direct SI in transporting O_3 down to the surface during winter could be related with the greater intensity of baroclinic systems [*James et al.*, 2003] which can favor the rapid descent into the troposphere of stratospheric air. The days selected by using the DIC showed an average O_3 increase of 8% with respect to the monthly running mean, while for days selected by less stringent criteria (indirect SI, mean time length 4 days) an average increase of 3% has been recorded. Nevertheless, despite their smaller O_3 enhancement in respect with direct events, because of their long duration and high-frequency indirect SI cannot be omitted to correctly assess the SI impact on tropospheric O_3.

[31] On the other hand, the contribution to tropospheric O_3 by direct SI could be overestimated if tropopause folds would affect the measurement area. In fact, from a purely dynamic point of view, the measurement site in the core of the fold would not be actually representative for the material quantity transported irreversibly into the troposphere by mixing processes on the edge of the folding [*Appenzeller and Davies*, 1992]. However, only tropopause folds going very deeply in troposphere (down to 2 km asl) could affect Mt. Cimone in this way. As these appear as extremely rare events (during our 6-year study, no tropopause below the 500 hPa level has been identified by the radiosoundings at the nearest S. Pietro Capofiume station), our analysis could be considered reasonably accurate.

[32] By using the methodology presented in *Elbern et al.* [1997] on daily values of O_3, ^7Be, RH and atmospheric pressure, we described an outline for SI in a mountain station. As evidenced in previous studies [*Davies and Schuepbach*, 1994; *Zanis et al.*, 1999; *Stohl et al.*, 2000] our analysis suggested that while indirect SI were mainly related to gradual downward motions in subsiding anticyclonic areas, direct SI were related to the passage of fronts over the region.

[33] As O_3 is one of the most important greenhouses gases [*Ramaswamy et al.*, 2001], the stratosphere-troposphere exchange can play a crucial role in the climate change. In fact, the high efficiency of SI in transporting stratospheric O_3 into the troposphere together with the relatively long O_3 lifetime in the free troposphere [*Liu et al.*, 1987] can contribute to increase O_3 concentrations in this region, where its radiative forcing is particularly efficient. Moreover, considering that future recovery of stratospheric O_3 and climate change will probably increase the O_3 downward flux [*Roelofs and Lelieveld*, 1997; *Butchart and Scaife*, 2001; *Collins et al.*, 2003], the extension and improvement of SI monitoring and studies appear as necessary steps.

[34] **Acknowledgments.** Part of this study is supported by ACCENT (GOCE-CT-2003-505337) and was part of EU-project STACCATO (EVK2-1999-00136), funded by the European Commission under Framework Programme IV, Environment and Climate. Part of the measurements was carried out during the EU-project VOTALP (ENV4-CT95-0025). We are grateful to S. Eckhardt, R. Damoah, P. James and N. Spichtinger for part of the ECMWF data handling. Radiosounding data were extracted by http://weather.uwyo.edu/upperair/sounding.html and http://raob.fsl.noaa.gov. NAO indexes were provided by the Climate Research Unit, UEA, Norwich, UK, and are available at http://www.cru.uea.ac.uk/cru/data/nao.htm. The authors are also grateful to the ''Ufficio Generale per la Meteorologia'' of the Italian Air Force and to P. Giambi, D. Amidei, and P. Amidei for the technical support at the ''O. Vittori''-Mt. Cimone station. Finally, the authors would like to thank an anonymous referee for his valuables comments.

References

Allen, D. J., J. E. Dibb, B. Ridley, K. E. Pickering, and R. W. Talbot (2003), An estimate of the stratospheric contribution to springtime tropospheric ozone maxima using TOPSE measurements and beryllium-7 simulations, *J. Geophys. Res.*, *108*(D4), 8355, doi:10.1029/2001JD001428.

Appenzeller, C., and H. C. Davies (1992), Structure of stratospheric intrusions into the troposphere, *Nature*, *358*, 570–572.

Arimoto, R., J. A. Snow, W. C. Graustein, J. L. Moody, B. J. Ray, R. A. Duce, K. K. Turekian, and H. B. Maring (1999), Influences of atmospheric transport pathways on radionuclide activities in aerosol particles from over the North Atlantic, *J. Geophys. Res.*, *104*(D17), 301–321.

Beekmann, M., G. Ancellet, and G. Megie (1994), Climatology of tropospheric ozone in southern Europe and its relation with potential vorticity, *J. Geophys. Res.*, *99*, 12,841–12,853.

Bithell, M., L. J. Gray, and B. D. Cox (1999), A three-dimensional view of the evolution of mid-latitude stratospheric intrusion, *J. Atmos. Sci.*, *56*, 673–688.

Bonasoni, P., F. Evangelisti, U. Bonafé, F. Ravegnani, F. Calzolari, A. Stohl, L. Tositti, O. Tubertini, and T. Colombo (1999), Stratospheric ozone intrusion episodes recorded at Mt. Cimone during VOTALP project: Case studies, *Atmos. Environ.*, *34*, 1355–1365.

Bonasoni, P., A. Stohl, P. Cristofanelli, F. Calzolari, T. Colombo, and F. Evangelisti (2000a), Background ozone variations at Mt. Cimone Station, *Atmos. Environ.*, *34*, 5183–5189.

Bonasoni, P., T. Colombo, P. Cristofanelli, F. Evangelisti, L. Tositti, O. Tubertini. U. Bonafè, F. Calzolari, and P. Giambi (2000b), Final report of CNR-ISAO, in *Vertical Ozone Transport in the Alps II-—Final Report*, pp. 87–96, Univ. of Agric. Sci., Inst. of Meteorol. and Phys., Vienna, Austria.

Butchart, N., and A. A. Scaife (2001), Removal of chlorofluorocarbons by increased mass exchange between the stratosphere and troposphere in a changing climate, *Nature*, *410*, 799–802.

Buzzi, A., G. Giovanelli, T. Nanni, and M. Tagliazucca (1985), Case study of stratospheric ozone descent to the lower troposphere during ALPEX, *Beitr. Phys. Atmos.*, *58*, 339–406.

Collins, W. J., R. G. Derwent, B. Garnier, C. E. Johonson, and M. G. Sanderson (2003), Effect of stratosphere-troposphere exchange on the future tropospheric ozone trend, *J. Geophys. Res.*, *108*(D12), 8528, doi:10.1029/2002JD002617.

Cristofanelli, P., et al. (2003), Stratosphere-to-troposphere transport: A model and method evaluation, *J. Geophys. Res.*, *108*(D12), 8525, doi:10.1029/2002JD002600.

Crutzen, P. J., M. G. Lawrence, and U. Poschl (1999), On the background photochemistry of tropospheric ozone, *Tellus, Ser. AB*, *51*, 123–146.

Danielsen, E. F. (1968), Stratospheric-tropospheric exchange based on radioactivity, ozone and potential vorticity, *J. Atmos. Sci.*, *25*, 502–518.

Davies, T. D., and E. Schuepbach (1994), Episodes oh high ozone concentrations at the Earth's surface resulting from transport down from the upper troposphere/lower stratosphere: A review and case studies, *Atmos. Environ.*, *28*, 53–68.

Defant, A. (1924), Schwankungen der atmospärischen Zirkulation über dem Nordatlantischen Ozean im 25-jährigen Zeitraum 1881–1905, *Geogr. Ann.*, *6*, 13–14.

Dutkiewicz, V. A., and L. Husain (1985), Stratospheric and tropospheric components of ^{7}Be in surface air, *J. Geophys. Res.*, *90*, 5783–5788.

Eisele, H., H. E. Scheel, R. Sladkovic, and T. Trickl (1999), High resolution lidar measurements of stratosphere-troposphere exchange, *J. Atmos. Sci.*, *56*, 319–330.

Elbern, H., J. Kowol, R. Sladkovic, and A. Ebel (1997), Deep stratospheric intrusions: A statistical assessment with model guided analysis, *Atmos. Environ.*, *31*, 3207–3226.

Ertel, H. (1942), Ein neuer hydrodynamischer Wirbelstaz, *Meteorol. Z.*, *59*, 277–281.

Feely, H. W., R. J. Larsen, and C. G. Sanderson (1989), Factors that cause seasonal variations in ^{7}Be concentrations in surface air, *J. Environ. Radioact.*, *9*, 223–249.

Feldmann, H., M. Memmesheimer, A. Ebel, P. Seibert, G. Wotawa, H. Kromp-Kolp, T. Trickl, and A. Prevot (1999), Evaluation of regional-scale model for the Alpine region with data from the VOTALP project, in *Proceedings of EUROTRAC-2 Symposium 98*, edited by P. M. Borrel and P. Borrel, pp. 478–482, WIT Press, Southampton, U. K.

Fischer, H., et al. (2003), Ozone production and trace gas correlations during the June 2000 MINATROC intensive measurement campaign at Mt. Cimone, *Atmos. Chem. Phys.*, *3*, 725–738.

Gauss, M., et al. (2003), Radiative forcing in the 21st century due to ozone changes in the troposphere and the lower stratosphere, *J. Geophys. Res.*, *108*(D9), 4292, doi:10.1029/2002JD002624.

Gerasopoulos, E., et al. (2001), A climatology of ^{7}Be at four high-altitude stations at the Alps and the northern Apennines, *Atmos. Environ.*, *35*, 6347–6360.

Gerasopoulos, E., C. S. Zerefos, C. Papastefanou, P. Zanis, and K. O'Brien (2003), Low frequency variability of beryllium-7 surface concentrations over the Eastern Mediterranean, *Atmos. Environ.*, *37*, 1745–1756.

Goering, M. A., W. A. Gallus Jr., M. A. Olsen, and J. L. Stanford (2001), Role of stratospheric air in a severe weather event: Analysis of potential vorticity and ozone, *J. Geophys. Res.*, *106*(D11), 11,813–11,823.

Hernández, F., J. Hernández-Armas, A. Catalán, J. C. Fernández-Aldecoa, and L. Karlsson (2005), Gross alpha, gross beta activities and gamma emitting radionuclides composition of airborne particulate samples in an oceanic island, *Atmos. Environ.*, *39*, 4057–4066.

Hoek, G., P. Fisher, B. Brunekreef, E. Lebret, P. Hofsschreuder, and M. G. Mennen (1993), Acute effects of ambient ozone on pulmunary function of children in the Netherlands, *Am. Rev. Respir. Dis.*, *147*, 11–117.

Hoerling, M. P., T. K. Schaack, and A. J. Lenzen (1991), Global objective tropopause analysis, *Mon. Weather Rev.*, *119*, 1816–1831.

Hurrell, J. W., G. Ottersen, Y. Kushnir, and M. Visbeck (2003), An overview of the North Atlantic Oscillation, in *The North Atlantic Oscillation: Climatic Significance and Environment Impact, Geophys. Monogr. Ser.*, vol. 134, pp. 1–35, AGU, Washington, D. C.

James, P., A. Stohl, C. Forster, S. Eckhardt, P. Seibert, and A. Frank (2003), A 15-year climatology of stratosphere-troposphere exchange with a Lagrangian particle dispersion model: 2. Mean climate and seasonal variability, *J. Geophys. Res.*, *108*(D12), 8522, doi:10.1029/2002JD002639.

Jones, P. D., T. Jonsson, and D. Wheeler (1997), Extension to the North Atlantic Oscillation using early instrumental pressure observations from Gibraltar and south-west Iceland, *Int. J. Climatol.*, *17*, 1433–1450.

Kinney, P. L. (1993), A meta-analysis of repeated FEV1 data from six summercamp studies: Mean effect of ozone and response heterogeneity, *Am. Rev. Respir. Dis.*, *147*, A636.

Koch, D. M., and M. E. Mann (1996), Spatial and temporal variability of ^{7}Be surface concentration, *Tellus, Ser. B*, *48*, 387–396.

Koch, D. M., D. J. Jacob, and W. C. Graustein (1996), Vertical transport of tropospheric aerosol as indicated by ^{7}Be and 210Pb in a chemical tracer model, *J. Geophys. Res.*, *101*, 18,651–18,666.

Lal, D., and B. Peters (1967), Cosmic ray produced radioactivity on the Earth, *Handb. Phys.*, *46*, 551–612.

Land, C., and J. Feichter (2003), Stratosphere-troposphere exchange in a changing climate simulated with the general circulation model MAECHAM4, *J. Geophys. Res.*, *108*(D12), 8523, doi:10.1029/2002JD002543.

Lee, H. N., G. Wan, X. Zheng, C. G. Sanderson, B. Josse, S. Wang, W. Yang, J. Tang, and C. Wang (2004), Measurements of ^{210}Pb and ^{7}Be in China and their analysis accompanied with global model calculations of ^{210}Pb, *J. Geophys. Res.*, *109*, D22203, doi:10.1029/2004JD005061.

Liu, S. C., M. Trainer, F. C. Fehsenfeld, D. D. Parrish, E. J. Williams, D. W. Fahey, G. Hubler, and P. C. Murphy (1987), Ozone production in the rural troposphere and the implications for regional and global ozone distributions, *J. Geophys. Res.*, *92*, 4191–4207.

Marshall, J., Y. Kushnir, D. Battisti, P. Chang, A. Czaja, R. Dickson, J. Hurrell, M. McCartney, R. Saravanan, and M. Visbeck (2001), North Atlantic climate variability: Phenomena, impacts and mechanisms, *Int. J. Climatol.*, *21*, 1863–1898.

Meloen, J., et al. (2003), Stratosphere-troposphere exchange: A model and method intercomparison, *J. Geophys. Res.*, *108*(D12), 8526, doi:10.1029/2002JD002274.

Olsen, M. A., W. A. Gallus, J. L. Stanford, and J. M. Brown (2000), Fine-scale comparison of TOMS total ozone data with model analysis of an intense Midwestern cyclone, *J. Geophys. Res.*, *105*, 20,487–20,498.

Poulida, O., R. R. Dickerson, and H. Heymsfield (1996), Stratosphere-troposphere exchange in a midlatitude mesoscale convective complex: 1. Observations, *J. Geophys. Res.*, *101*(D3), 6823–6836.

Ramaswamy, V., O. Boucher, J. Haigh, D. Hauglustaine, J. Haywood, G. Myhre, T. Nakajima, G. Y. Shi, and S. Salomon (2001), Radiative forcing of climate change, in *Climate Change 2001: The Scientific Basis—Contribution of Working Group I to the Third Assessment Report of The Intergovernmental Panel on Climate Change*, edited by J. T. Houghton et al., pp. 349–416, Cambridge Univ. Press, New York.

Reed, R. J. (1955), A study of a characteristic type of upper-level frontogenesis, *J. Met.*, *12*, 226–237.

Reiter, R., K. Munzert, H. J. Kanter, and K. Poetzl (1983), Cosmogenic radionuclides and ozone at a mountain station at 3.0 km a.s.l., *Arch. Meterol. Geophys. Bioklimatol., Ser. B*, *32*, 131–160.

Roelofs, G.-J., and J. Lelieveld (1997), Model study of the influence of cross-tropopause O_3 transports on tropospheric O_3 levels, *Tellus, Ser. B*, *49*, 38–55.

Scheel, H. E. (2002), Measurements of O_3, ^{7}Be, RH and CO at the Zugspitze summit, *STACCATO—Final Report*, pp. 58–62, Lehrstuhl für Bioklimatol. und Immissionsforsch., Tech. Univ. München, Munich, Germany.

Scheel, H. E., R. Sladkovic, and H. J. Kanter (1999), Ozone variations at the Zugspitze (2962 m a.s.l.) during 1996–1997, in *Proceeding of EUROTRAC-2 Symposium 1998*, edited by P. M. Borrel and P. Borrel, pp. 260–263, WIT Press, Southampton, U. K.

Schuepbach, E., T. D. Davies, and A. C. Massacand (1999), An unusual springtime ozone episode at high elevation in the Swiss Alps: Contributions both from cross-tropopause exchange and from the boundary layer, *Atmos. Environ.*, *33*, 1735–1744.

Slàdkovic, R., and K. Munzert (1990), Lufthygienisc-klimatologische Uberwachung im bayrischen Alpenarum, *IFU Rep. 908080,* Abschlussbericht, Abschnitt VI/4, Fraunhofer Inst. for Atmos. Environ. Res., Garmisch-Partenkirchen, Germany.

Sprenger, M., and H. Wernli (2003), A Northern Hemispheric climatology of cross-tropopause exchange for the ERA15 time period (1979–1993), *J. Geophys. Res.*, *108*(D12), 8521, doi:10.1029/2002JD002636.

Staehelin, J., J. Thudium, R. Buheler, A. Volz-Thomas, and W. Graber (1994), Trends in surface ozone concentrations at Arosa (Switzerland), *Atmos. Environ.*, *28*, 75–78.

Stohl, A., G. Wotawa, P. Seibert, and H. Kromp-Kolb (1995), Interpolation errors in wind field as a function of spatial and temporal resolution and their impact on different types of kinematic trajectories, *J. Appl. Meteorol.*, *34*, 2149–2165.

Stohl, A., N. Spichtinger-Rakowsky, P. Bonasoni, H. Feldmann, M. Memmesheimer, H. E. Scheel, T. Trickl, S. Hubener, W. Ringer, and M. Mandl (2000), The influence of stratospheric intrusions on alpine ozone concentrations, *Atmos. Environ.*, *34*, 1323–1354.

Sudo, K., Y. Masaaki, and H. Akimoto (2003), Future changes in stratosphere-troposphere exchange and their impacts on future tropospheric ozone simulations, *Geophys. Res. Lett.*, *30*(24), 2256, doi:10.1029/2003GL018526.

Thornes, J. E., and D. B. Stephenson (2001), How to judge the quality and value of weather forecast products, *Meteorol. Appl.*, *8*, 307–314.

Tositti, L., S. Hübener, H. J. Kanter, W. Ringer, S. Sandrini, and L. Tobler (2004), Intercomparison of sampling and measurement of ^{7}Be in air at four high-altitude locations in Europe, *Appl. Radiat. Isotopes*, *61*, 1497–1502.

Trigo, I. F., G. R. Bigg, and T. D. Davies (2002), Climatology of cyclogenesis mechanism in the Mediterranean, *Mon. Weather Rev.*, *130*, 549–569.

U.S. Department of Commerce (1976), *Radiosonde Code, Fed. Meteorol. Handb.*, vol. 4, Washington, D. C.

Vaughan, G., and J. D. Price (1989), Ozone transport into the troposphere in a cut-off low event, in *Ozone in the Atmosphere*, edited by R. D. Bojkov and P. Fabian, pp. 415–416, Deepak, A., Hampton, Va.

Volz-Thomas, A., et al. (2002), Tropospheric ozone and its control, in *Towards Cleaner Air for Europe-Science, Tools and Applications. Part 1: Results from the EUROTRAC-2; Synthesis and Integration (S&I) Project*, edited by P. J.-H. Builtjes et al., chap. 3, pp. 73–122, Int. Sci. Secr., Munich, Germany.

Yenger, J. J., A. A. Klonecky, H. Levy II, W. J. Moxim, and G. R. Carmichael (1999), An evaluation of chemistry's role in the winter-spring ozone maximum found in the northern midlatitude free troposphere, *J. Geophys. Res.*, *104*, 3655–3667.

Wallace, J. M., and D. S. Gutzler (1981), Teleconnections in the geopotential height field during Northern Hemisphere winter, *Mon. Weather Rev.*, *109*, 784–812.

Wotawa, G., H. Kroger, and A. Stohl (2000), Transport towards the Alps—Results from trajectory analyses and photochemical model studies, *Atmos. Environ.*, *34*, 1367–1377.

Zanis, P., E. Schuenpbach, H. W. Gaeggeler, S. Huebener, and L. Tobler (1999), Factors controlling beryllium-7 at Jungfraujoch in Switzerland, *Tellus*, *51*(4), 789–805.

Zanis, P., et al. (2003), Forecast, observation and modelling of a deep stratospheric intrusion event over Europe, *Atmos. Chem. Phys.*, *3*, 763–777.

U. Bonafè, P. Bonasoni, F. Calzolari, P. Cristofanelli, and F. Evangelisti, National Research Council, Institute of Atmosphere and Climate Sciences, I-40129, Bologna, Italy. (p.cristofanelli@isac.cnr.it)

S. Sandrini and L. Tositti, Environmental Radiochemistry Laboratory, Chemistry Department, Bologna University, I-40126, Bologna, Italy.

A. Stohl, Norsk Institutt for Luftforskning, N-2027 Kjeller, Norway.